Acta Biochimica Polonica

Vol. 54 No. 4/2007, 769–775

on-line at: www.actabp.pl

Regular paper

^{15}N magnetic relaxation study of backbone dynamics of the ribosome-associated cold shock response protein Yfia of *Escherichia coli*★

Igor Zhukov[1,2], Peter Bayer[3], Beate Schölermann[3*] and Andrzej Ejchart[1]✉

[1]*Institute of Biochemistry and Biophysics, Polish Academy of Sciences, Warszawa, Poland;* [2]*Slovenian NMR Centre, National Institute of Chemistry, Ljubljana, Slovenia;* [3]*Department of Structural and Medicinal Biochemistry, Centre of Medical Biotechnology, University of Duisburg-Essen, Essen, Germany*

Received: 25 July, 2007; revised: 02 October, 2007; accepted: 26 October, 2007;
available on-line: 31 October, 2007

In the solution structure of the ribosome-associated cold shock response protein Yfia of *Escherichia coli* in the free state two structural segments can be distinguished: a well structured, rigid N-terminal part displaying a βαββββα topology and a flexible C-terminal tail comprising last 20 amino-acid residues. The backbone dynamics of Yfia protein was studied by ^{15}N nuclear magnetic relaxation at three magnetic fields and analyzed using model-free approach. The overall diffusional tumbling of the N-terminal part is strongly anisotropic with a number of short stretches showing increased mobility either on a subnanosecond time scale, or a micro- to millisecond time scale, or both. In contrast, the unstructured polypeptide chain of the C-terminal part, which cannot be regarded as a rigid structure, shows the predominance of fast local motions over slower ones, both becoming faster closer to the C-terminus.

Keywords: ^{15}N NMR spectroscopy, model-free approach, stress adaptation, protein Y, anisotropic overall molecular diffusion, disordered polypetide chain motion

INTRODUCTION

Living organisms react to the rapidly changing environmental conditions with the production of specialized stress factors while limiting the ribosomal synthesis of most metabolic proteins. Recently, a ribosome-related mechanism of cold shock adaptation has been elucidated in *Escherichia coli* (Agafonov *et al*., 1999; 2001). Ribosomes, which serve as fundamental checkpoints for sensing changes in nutrient level and in temperature, are composed of two subunits (30S and 50S) that undergo a cycle of association and dissociation during protein synthesis. A sudden drop in temperature causes the bacterium to initiate the production of protein Yfia (protein Y, PY) which instantly associates with the 30S ribosomal subunit while blocking the tRNA- and mRNA-binding channel. Upon cold shock Yfia competes with translation initiation factors IF1 and IF3 that are required for the dissociation of ribosomal subunits (Vila-Sanjurjo *et al*., 2004). Formation of the Yfia–30S complex provides a storage mechanism for intact 70S ribosomes and allows their rapid reactivation on improving environmental conditions.

Variants of protein Y are widely dispersed in bacteria but homologous proteins can also be found in chloroplasts of plants such as *Spinacia oleracea* (PSrp-1) (Johnson *et al*., 1990; Agafonov *et al*., 1999). Members of the protein Y family are generally thought to be involved in the process of adaptation

★This paper is dedicated to Professor Tadeusz Chojnacki from the Institute of Biochemistry and Biophysics, Polish Academy of Sciences in Warsaw on the occasion of the 50th anniversary of his scientific activity and 75th birthday.

✉Correspondence to: Andrzej Ejchart, Institute of Biochemistry and Biophysics, Polish Academy of Sciences, A. Pawińskiego 5A, 02-106 Warszawa, Poland; phone: (48) 22 592 2037; fax: (48) 22 658 4683; e-mail: aejchart@ibb.waw.pl

*Currently at the Max-Planck Institute for Molecular Physiology, Dortmund, Germany

Abbreviations: CPMG, Carr-Purcell-Meiboom-Gill sequence; GARP sequence, Globally optimized Alternating-phase Rectangular Pulses; HSQC, heteronuclear single quantum correlation; MFA, model-free approach; NMR, nuclear magnetic resonance; NOE, nuclear Overhauser effect; NOESY, nuclear Overhauser effect spectroscopy.

to changing enviromental conditions. Recently, two solution structures of protein Y from *E. coli* (Kalinin *et al*., 2002; Ye *et al*., 2002; Rak *et al*., 2002) and one from the bacteria *Haemophilus influenzae* (Parsons *et al*., 2001) as well as the crystal structure of a complex of Yfia bound to the *E. coli* 30S ribosomal subunit (11 Å resolution) (Vila-Sanjurjo *et al*., 2004) have been published revealing the structural basis for the control of translation initiation. The protein structure resembles a βαββββα folding topology and represents a compact two layered sandwich of two nearly parallel α-helices packed against the same side of a four-stranded β-sheet (Fig. 1). Since the C-terminal 20 amino acids are flexible in solution, the ribosome-bound structure was determined by docking a truncated model of protein Y lacking this region into the average electron density. In the crystal complex Yfia resides in close proximity to 16S rRNA residues which are known to be universally conserved markers for the A and P sites. Bases G926, C1400, C1402 and A1493 are protected by the positively charged side chains of amino acids R22, K25, K28, K79, R82 and K86 of Yfia. These residues block tRNA from the A-site and inhibit binding of deacetylated tRNA to the P-site.

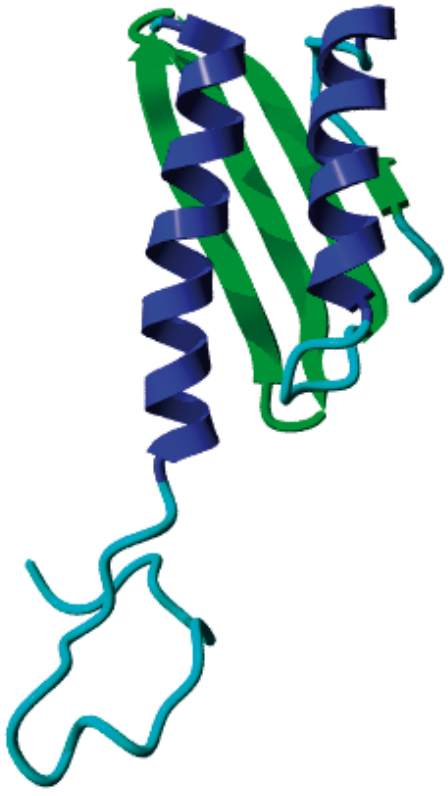

Figure 1. Ribbon representation of the Yfia protein structure (Rak *et al*., 2002).
α-Helices are marked in blue, β-strands in green. The model was created and visualized with the programs YASARA 5.1.25 (www.yasara.org) and PovRay 3.6 (www.povray.org).

Recently the relationship between the internal dynamics of macromolecules and their biological functions has been the subject of much research (Palmer, 2004; Kay, 2005). Information about the dynamics of a protein backbone from ^{15}N NMR relaxation studies is typically based on the measurements of ^{15}N longitudinal (R_1) and transverse (R_2) relaxation rates and the steady-state ^{1}H-^{15}N nuclear Overhauser enhancement ({^{1}H}-^{15}N *NOE*) giving access to the mobility of N–H vectors (Korzhnev *et al*., 2001). Owing to the complexity of motions in proteins a specific type of motion was seldom assumed and the experimental data have been usually analyzed by the model-free approach (MFA) (Lipari & Szabo, 1982). Analysis of relaxation data reveals that, with the exception of loops and termini, protein backbone motions in native conformation are severely restricted on the nanosecond timescale. On the other hand, the backbone motions of partially folded proteins usually show a significant contribution of motions with the timescale comparable to or slower than the overall correlation time (Alexandrescu & Shortle, 1994; Brutscher *et al*., 1997; Ochsenbein *et al*., 2004).

MATERIALS AND METHODS

Sample preparation. *E. coli* DNA encoding Yfia (sequence available in the SwissProt DataBank; entry code: YFIA_ECOLI; accession number P11285) was cloned into the vector pET11c. After transfection in BL21(DE3) the protein was expressed and purified as described earlier (Kalinin *et al*., 2002). A typical NMR sample contained 50 mM KH_2PO_4 buffer, 50 mM LiCl and 10% (v/v) D_2O, with a pH of 6.8 and the protein concentration of 0.8 mM.

NMR experiments. NMR data were recorded at 300 K on a Varian INOVA 400, a Varian UNITY+ 500 and a Varian INOVA 600 spectrometers at 9.4, 11.7, and 14.1 T, respectively. Longitudinal (R_1) and transverse (R_2) relaxation rates were measured at three magnetic field strengths using a sensitivity enhanced [^{15}N-^{1}H] HSQC pulse sequence (Kay *et al*., 1992a) with the option of either R_1 or R_2 measurements of ^{15}N nuclei (Farrow *et al*., 1994). In the case of R_1 twelve evolution times within the range 10–1450 ms were used. The R_2 relaxation rate measurements were performed with the Carr-Purcell-Meiboom-Gill (CPMG) pulse train. Refocusing time of 650 μs was used and eight evolution times covered the range 10–250 ms. The acquisition parameters for R_1 and R_2 measurements were identical with the exception of the delay between π (^{1}H) pulses used for the cross-correlation effect suppression (Kay *et al*., 1992b). Delays of 5 ms and 10 ms were used in R_1 and R_2 measurements, respectively. The relaxation delay of 2.5 s was employed in both experiments.

{^{1}H}-^{15}N *NOE*s were measured at 9.4 and 11.7 T with a pulse sequence included in the ProteinPack Varian Inc. (Palo Alto, USA) software. The relaxation delay of 7 s and ^{1}H saturation of 3 s were employed. Standard *NOE* measurement (spectra with and without ^{1}H saturation) was performed at 9.4 T, whereas the dynamic variant of the experiment was chosen for the *NOE* determination at 11.7 T (Zhukov & Ejchart, 1999). ^{1}H saturation time was set to 0.1, 0.15, 0.3, 0.7, 1.3, and 2.1 s. In all relaxation measurements ^{15}N decoupling during the acquisition was applied using the GARP sequence with $\gamma B_2/2\pi$ = 3200 Hz (Shaka *et al*., 1985). All spectra were processed by the NMRPipe (Delaglio *et al*., 1995) and analyzed by the XEASY (Bartels *et al*., 1995) programs. Relaxation parameters were determined by the two-parameter nonlinear least-squares fit of cross-peak heights to a single exponential decay. Errors in the determination of the relaxation rates were obtained from the covariance matrix. Error in the *NOE* values was estimated from assuming that the uncertainty in the peak heights in the spectra recorded with and without ^{1}H saturation was equal to rms noise in each of these two spectra (Tjandra *et al*., 1995).

Analysis of relaxation data. Two relaxation mechanisms have to be taken into account for the nuclear spin relaxation of amide nitrogens in proteins: the chemical shift anisotropy of a nitrogen nucleus and the dipole–dipole interaction between a nitrogen and the hydrogen directly bound to it. Equations describing relaxation parameters in terms of spectral density functions are given as (Korzhnev *et al*., 2001):

$$R_1 = \frac{1}{4}D^2\left[J(\omega_H-\omega_N)+3J(\omega_N)+6J(\omega_H+\omega_N)\right]+\frac{1}{3}C^2J(\omega_N)$$

$$R_2 = \frac{1}{8}D^2\left[4J(0)+J(\omega_H-\omega_N)+3J(\omega_N)+6J(\omega_H)+6J(\omega_H+\omega_N)\right]+$$
$$+\frac{1}{18}C^2\left[4J(0)+3J(\omega_N)\right]+R_{ex}$$

$$NOE = 1+\left(\frac{\gamma_H}{\gamma_N}\right)\frac{D^2}{4R_1}\left[6J(\omega_H+\omega_N)-J(\omega_H-\omega_N)\right]$$

where $D=\frac{\mu_0}{4\pi}\frac{\gamma_N\gamma_H\hbar}{\langle r_{NH}^3\rangle}$, $C = \omega_N\Delta\sigma$ and other symbols have their usual meaning. In further calculations the values of N–H distance, r_{NH} = 0.104 nm (Case, 1999), and ^{15}N chemical shift anisotropy, $\Delta\sigma$ = –170 ppm (Tjandra *et al*., 1996a; 1996b), were used. The additional term R_{ex} takes into account the conformational exchange contribution to R_2 resulting from processes in the micro- to millisecond time scale often named the chemical exchange effect (Stone *et al*., 1992; Korzhnev *et al*., 2001). Such processes, slower than the molecular tumbling, but fast enough to average chemical shifts, can influence transverse relaxation rates determined using the CPMG method. The R_{ex} contribution to the transverse relaxation rate is proportional to the square of the chemical shift difference between exchanging states, $\Delta\delta$, and ω_N — the Larmor frequency at the fast exchange limit. It should be pointed out that conformational exchange mechanism is able to participate in the transverse relaxation only if $\Delta\delta \neq 0$. This term can be written as $R_{ex} = \Phi\omega_N^2$ (Peng & Wagner, 1995). The proportionality factor Φ represents the effectiveness of conformational exchange processes.

Model-free approach spectral density function takes the form (Lipari & Szabo, 1982):

$$J(\omega) = \frac{2}{5}\left[\frac{S^2\tau_R}{1+(\omega\tau_R)^2}+\frac{(1-S^2)\tau}{1+(\omega\tau)^2}\right]$$

with $\tau^{-1} = \tau^{-1}_R + \tau^{-1}_{int}$. The isotropic overall motion is described by the correlation time τ_R and internal motion(s) by a generalized order parameter S which is a measure of the degree of spatial restriction of the motion and an effective correlation time τ_{int} corresponding to the rate of this motion.

In the case of anisotropic overall motion the spectral density function becomes more complex. Combining the model-free approach with axially anisotropic overall tumbling (Woessner, 1962) the spectral density function takes the form (Barbato *et al*., 1992):

$$J(\omega) = \sum_{k=1}^{3} A_k(\alpha)J_{MFA}(S,\tau_k,\tau_{i,k};\omega)$$

where α is the angle between the N–H vector and the unique axis of the rotational diffusion tensor. Coefficients $A_k(\alpha)$ have the form:

$A_1 = 0.75(\sin^4\alpha)$, $A_2 = 3(\sin^2\alpha)(\cos^2\alpha)$,
$A_3 = 0.25(3\cos^2\alpha - 1)$

The overall correlation times τ_k are defined as:

$$\tau_1 = 1/(4D_{||}+2D_{\perp}),\quad \tau_2 = 1/(D_{||}+5D_{\perp}),\quad \tau_3 = 1/(6D_{\perp})$$

and the effective correlation times $\tau_{i,k}$ are as follows: $\tau^{-1}_{i,k} = \tau^{-1}_k + \tau^{-1}_{int}$.

$D_{||}$ and $D_{\perp}$ are parallel and perpendicular components of the rotational diffusion tensor. Additional two parameters, the polar angles θ and φ, relate the direction of the unique axis of the diffusion tensor to the molecule fixed coordinate system. The geometric coefficients $A_k(\alpha)$ were calculated using the atomic coordinates of the NMR-derived structure of Yfia (PDB accession no. 1N3G).

Least-squares procedure used to optimize the model parameters consisted of a minimization through a grid-search of the target function χ given by:

$$\chi = \sum_{i=1}^{8}\sum_{j=1}^{N}[(P_{ij,\exp}-P_{ij,calc})^2/\sigma_{ij}^2]$$

where the sum was over eight relaxation parameters (R_1s and R_2s at three magnetic field strengths and *NOE*s at two magnetic field strengths) for each of N residues, and $P_{ij,calc}$ were the appropriate relaxation parameters calculated from the assumed model. The σ_{ij} values were the corresponding standard deviations of experimentally derived $P_{ij,exp}$. The minimization procedure delivered four global parameters $D_{||}$, $D_{\perp}$, θ, φ and N sets of local parameters S^2_j, $\tau_{j,int}$, and Φ_j. Model parameter uncertainties derived in the minimization of target function were obtained as standard deviations from 200 Monte Carlo simulations (Press *et al.*, 1986).

RESULTS AND DISCUSSION

Resonance assignments of ^{15}N nuclei in Yfia protein have been published recently (Kalinin *et al.*, 2002). Eight ^{15}N relaxation parameters P_{exp} were measured for 98 backbone amide groups out of 113 residues. The lacking data comprise the N-terminal M1, four prolines (P14, P37, P45, P57), stretch of residues Q31–I35 showing extremely weak correlations, and five other residues with strongly superposed crosspeaks (T2, M3, I5, A94, A104). A graphic representation of the relaxation parameters is presented in Fig. 2 and the actual values are given in the Supplementary Material. All relaxation parameters show the expected dependence on the magnetic field strength: the R_1s decrease whereas R_2s and *NOE*s increase with B_0. The negative *NOE* and markedly smaller R_2 values observed for the C-terminal part of the protein are typical for unstructured protein segments (Alexandrescu & Shortle, 1994). Analysis of the ^{15}N relaxation data was carried out separately for the well-structured N-terminal part (residues 1–91) and the flexible, unstructured C-terminal part (residues 92–113).

N-terminal part of Yfia protein

The MFA with anisotropic overall motion was applied to analyse the dynamics of the N-terminal part of Yfia protein. Relaxation data for 78 residues were fitted simultaneously without any arbitrary omission of residues displaying deviations of R_2/R_1 ratios from the average and/or smaller *NOE*s (Clore *et al.*, 1990). The model included global parameters $D_{||}$, $D_{\perp}$, θ, and φ, as well as local, residue-specific parameters, S^2, τ_{int}, and Φ.

Rotational diffusion constants are equal to: $D_{||} = (1.05 \pm 0.05)\ 10^7\ s^{-1}$ and $D_{\perp} = (2.30 \pm 0.08)\ 10^7\ s^{-1}$. The anisotropy of the overall motion is considerable with the anisotropy ratio $D_{||}/D_{\perp} = 0.46$. An effective correlation time $\tau_{R,eff} = 1/(2D_{||} + 4D_{\perp}) = 8.8$ ns (Barbato *et al.*, 1992) fits well the value expected for a 113-residue protein.

A graphic representation of the model-free approach parameters obtained for the anisotropic model is given in Fig. 3. The S^2 values are related to the local mobility of the N–H vectors on the subnanosecond timescale. For a completely restricted local motion $S^2 = 1$, whereas $S^2 = 0$ corresponds to fully unrestricted motion. Secondary structure segments show uniform, large S^2 values which decrease at their ends. This effect is especially well visible for the C-terminal residue of helix α_2, H90, which can hardly be included in a rigid structural element on the basis of its S^2 value.

Residues in turns between β_2–β_3 and β_3–β_4 display increased mobility on the ns–ps time scale (smaller S^2 values) in contrast to those between the β_4–α_2 secondary structure elements. The loop between β_1–α_1 shows dispersion of S^2 values, whereas a lack of experimental data precludes any firm conclusion concerning fast motion mobility in the α_1–β_2 loop. Nevertheless, small S^2 values for W30 (S^2 = 0.74) and N36 (S^2 = 0.58) may point to an increased amplitude of fast local motions in this area.

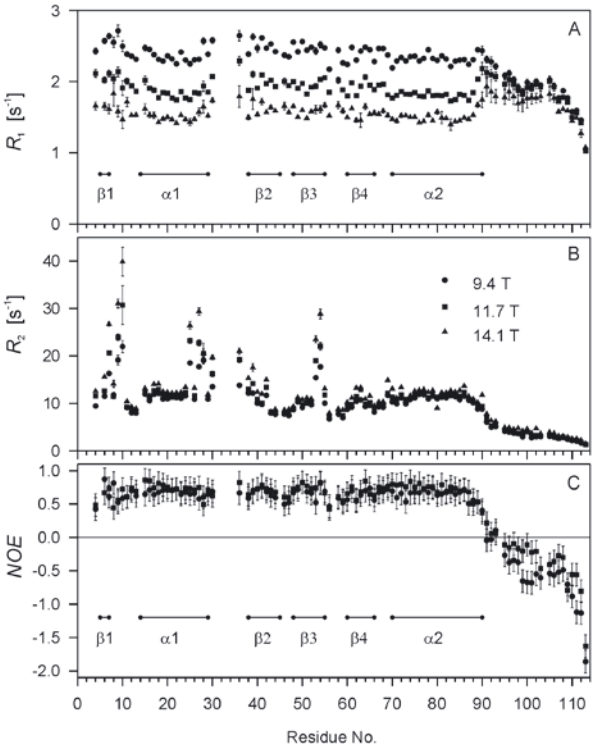

Figure 2. Relaxation data as a function of Yfia protein structure.
A — R_1s, B — R_2s, and C — *NOE*s. Error bars correspond to standard deviations of data points in individual fits. Errors of the *NOE* values at 9.4 T were estimated as described by Alexandrescu and Shortle (1994). Data were obtained at 9.4 T (●), 11.7 T (■), and 14.1 T (▲). Structure elements are represented by horizontal lines.

The Φ parameter represents slow, often large-scale conformational motions, on the ms–μs time scale comprising several adjacent residues (Korzhnev *et al*., 2001). Several such areas showing elevated Φ values can be found in the N-terminal part of Yfia protein; residues 4–10 comprising β_1 and a part of the following loop, residues 25–30 and 36 constituting the C-end of α_1 and the following turn, residues 53–55 constituting the C-end of β_3. Residues 38–42 corresponding approximately to β_2 and residues 60–72 comprising β_4 and the β_4–α_2 turn also display small but uniform conformational exchange effects. On the basis of the large Φ values for residues W30 and N36 one may speculate that the extremely weak correlations for residues Q31–I35 precluding determination of their relaxation parameters are due to the conformational exchange not fast enough to fully average chemical shifts and resulting in strong broadening of the resonances (Cavanagh *et al*., 1996).

In fact, a significant number of residues forming the four-stranded β-sheet show a significant amount of slow conformational motions allowing us to conclude that its bigger part undergoes relatively slow, large-scale conformational motion. One can speculate that this conformational flexibility is characteristic only for free Yfia protein and it is probably suppressed when the protein is associated with the ribosome.

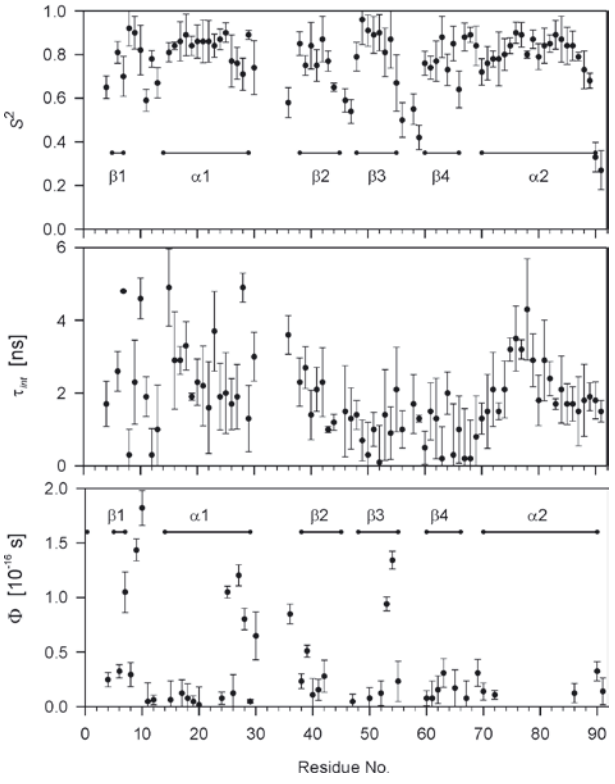

Figure 3. Order parameters S^2, correlation times of internal motions τ_{int}, and Φ factors characterizing conformational exchange processes along the sequence of N-terminal part of Yfia protein (amino-acid residues 1–91).
Error bars represent appropriate standard deviations obtained from Monte Carlo simulations. Structure elements are represented by horizontal lines.

In the N-terminal part of Yfia protein increased mobility on the ns–ps timescale often goes together with the increased mobility on the ms–μs timescale. Many residues, especially in turns, show both small S^2 values and large Φ values indicating extremely high mobility of those parts of the protein in a free state.

A short comment should be given on the values of correlation times for internal motions, τ_{int}. Many of them seem to be unexpectedly large and becoming of the same order of magnitude as the effective overall correlation time. Nevertheless, one should take into account that τ_{int} are the most prone of all local MFA parameters (S^2, τ_{int}, Φ) to experimental inaccuracies. This feature is reflected by the large error bars in the central part of Fig. 3. Equally important is that τ_{int} values are sensitive to the assumed values of r_{NH} and $\Delta\sigma$ used in calculations. For instance, use of $r_{NH} = 0.102$ nm instead of 0.104 nm could decrease τ_{int} values on average 2.7 times. In general, the pattern of τ_{int} follows that of S^2. Less local freedom corresponds to longer τ_{int}s and this regularity seems to be self-explanatory.

C-terminal part of Yfia protein

Since the unstructured, flexible C-terminal part cannot be regarded as a rigid rotor, a description of its motion in terms of a single overall correlation time may not be appropriate. In such a case the motion of the N–H vector in the *l*-th residue can be described by the model-free approach spectral density functions wherein the global parameter τ_R is substituted with a local one, $\tau_{R,l}$. (Alexandrescu & Shortle, 1994; Brutscher *et al*., 1997). Alternatively, the use of a distribution of correlation times allows one to account for intramolecular motions comparable to or slower than overall molecular tumbling (Ochsenbein *et al*., 2002). A number of models utilizing different distribution functions have been used for the interpretation of nuclear relaxation data in synthetic polymers (Ward & Klein, 1996) and polypeptide chains (Buevich *et al*., 2001). Since the model utilizing local correlation times describes well the dynamics of an unstructured tail attached to a fully folded fragment — the case of Yfia protein — we used it in the analysis of the ^{15}N relaxation data of the C-terminal part of the protein. The results are shown in Fig. 4. Φ values are equal to zero within the accuracy limit and are not included. S^2 values are much smaller than those in the N-terminal part (except residues 90 and 91) pointing to the high preference of fast local motions characterized by τ_{int}

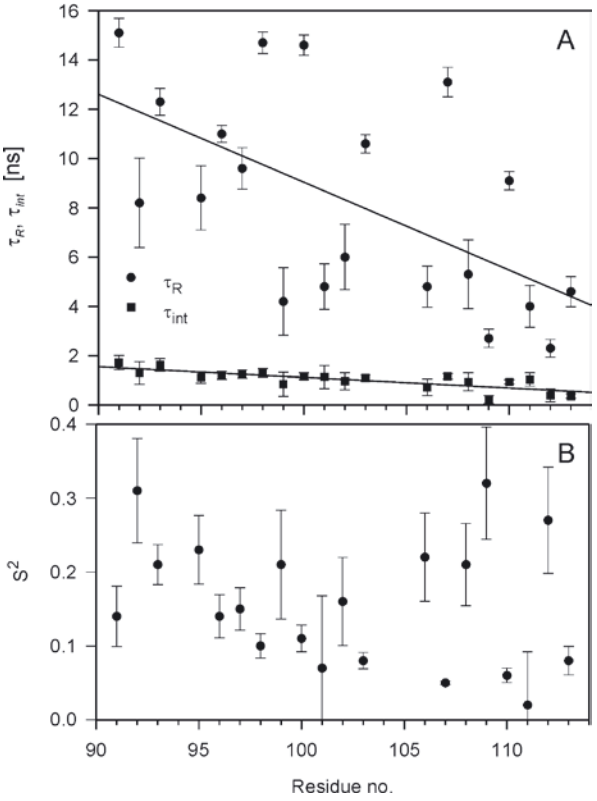

Figure 4. Residue-specific correlation times, $\tau_{R,i}$ (●) and τ_{int} (■), (A) and order parameters (B) obtained for C-terminal part of Yfia protein (amino-acid residues 91–113). Error bars represent appropriate standard deviations obtained from Monte Carlo simulations. Regression lines in part A correspond to correlation coefficients: $r = 0.59$ for $\tau_{R,i}$ and $r = 0.79$ for τ_{int}.

over the slower motions described by $\tau_{R,l}$. Since the N-domain anchors the unstructured C-domain, the systematic decrease of both correlation times when approaching the C-terminus reflects the increasing amount of conformational freedom. It strongly supports the conclusion that the C-terminus is unstructured and randomly changes its conformation. The MFA parameters calculated for residues A104–E108, which showed a number of cross peaks characteristic for a helix in NOESY spectra (Ye *et al*., 2002), do not reflect any increase of conformational stiffness for these residues.

CONCLUSION

The backbone dynamics of Yfia protein is strongly diversified. The overall tumbling of the rigid N-terminal part comprising 91 amino-acid residues is typical for native proteins, whereas the intense local motions within the C-terminal part (22 amino-acid residues) are characteristic for unstructured or denaturated proteins. A simultaneous appearance of so different dynamic behaviours in the same protein molecule is very unusual.

Although the role of Yfia dynamics on the translation inhibition by directly blocking the P-site of the ribosome seems to be minor, it might play a crucial role in the dissociation of protein Y from the ribosome under elevated temperatures (37°C). The slow conformational motion within the N-terminus might be reduced under cold shock allowing strong binding of protein Y to the ribosomal subunit. Under elevated temperatures the internal motion may weaken the binding to the ribosom allowing the competitive binding of initiation factor IF1 to an overlapping binding site. However, the role of the C-terminus is unknown. Its high internal dynamic and flexibility suggest an unknown binding partner.

Acknowledgements

P.B. thanks the Max-Planck-Society for financial support.

REFERENCES

Agafonov DE, Kolb VA, Nazimov IV, Spirin AS (1999) A protein residing at the subunit interface of the bacterial ribosome. *Proc Natl Acad Sci USA* **96**: 12345–12349.

Agafonov DE, Kolb VA, Spirin AS (2001) Ribosome-associated protein that inhibits translation at the aminoacyl-tRNA binding stage. *EMBO Rep* **2**: 399–402.

Alexandrescu AT, Shortle D (1994) Backbone dynamics of a highly disordered 131 residue fragment of staphylococcal nuclease. *J Mol Biol* **242**: 527–546.

Barbato G, Ikura M, Kay LE, Pastor RW, Bax A (1992) Backbone dynamics of calmodulin studied by ^{15}N relaxation using inverse detected two-dimensional NMR spectroscopy: the central helix is flexible. *Biochemistry* **31**: 5269–5278.

Bartels C, Xia T, Billeter M, Güntert P, Wüthrich K (1995) The program XEASY for computer-supported NMR spectral analysis of biological macromolecules. *J Biomol NMR* **5**: 1–10.

Brutscher B, Brüschweiler R, Ernst RR (1997) Backbone dynamics and structural characterization of the partially folded A state of ubiquitin by ^{1}H, ^{13}C, and ^{15}N nuclear magnetic resonance spectroscopy. *Biochemistry* **36**: 13043–13053.

Buevich AV, Shinde UP, Inouye M, Baum J (2001) Backbone dynamics of the natively unfolded pro-peptide of subtilisin by heteronuclear NMR relaxation studies. *J Biomol NMR* **20**: 233–249.

Case DA (1999) Calculations of NMR dipolar coupling strengths in model peptides. *J Biomol NMR* **15**: 95–102.

Cavanagh J, Fairbrother WJ, Palmer III AG, Skelton NJ (1996) *Protein NMR spectroscopy. Principles and practice;* pp 290–297. Academic Press, San Diego, London.

Clore GM, Driscoll PC, Wingfield PT, Gronenborn AM (1990) Analysis of backbone dynamics of interleukin-1β using two-dimensional inverse detected heteronuclear ^{15}N-^{1}H NMR spectroscopy. *Biochemistry* **29**: 7387–7401.

Delaglio F, Grzesiek S, Vuister GW, Zhu G, Pfeifer J, Bax A (1995) A multidimensional spectral processing system based on UNIX pipes. *J Biomol NMR* **6**: 277–293.

Farrow NA, Muhamdiram R, Singer AU, Paskal SM, Kay CM, Gish G, Shoelton SE, Pawson T, Forman-Kay JD, Kay LE (1994) Backbone dynamics of a free and a phosphopeptide-complexed *Src* homology 2 domain studied by ^{15}N NMR relaxation. *Biochemistry* **33**: 5984–6003.

Johnson CH, Kruft V, Subramanian AR (1990) Identification of a plastid-specific ribosomal protein in the 30S subunit of chloroplast ribosomes and isolation of the cDNA clone encoding its cytoplasmic precursor. *J Biol Chem* **265**: 12790–12795.

Kalinin A, Rak A, Scherbakov D, Bayer P (2002) ^{1}H, ^{13}C and ^{15}N resonance assignments of the ribosome-associated cold shock response protein Yfia of *Escherichia coli*. *J Biomol NMR* **23**: 335–336.

Kay LE (2005) NMR studies of protein structure and dynamics. *J Magn Reson* **173**: 193–207.

Kay LE, Keifer P, Saarinen T (1992a) Pure absorption gradient enhanced heteronuclear single quantum correlation spectroscopy with improved sensitivity. *J Am Chem Soc* **114**: 10663–10665.

Kay LE, Nicholson LK, Delaglio F, Bax A, Torchia DA (1992b) Pulse schemes for removal of the effects of cross-correlation between dipolar and chemical-shift anisotropy relaxation mechanisms on the measurement of heteronuclear T_1 and T_2 values in proteins. *J Magn Reson* **97**: 359–375.

Korzhnev DM, Billeter M, Arseniev AS, Orekhov Y (2001) NMR studies of Brownian tumbling and internal motions in proteins. *Prog NMR Spectr* **38**: 197–266.

Lipari G, Szabo A (1982) Model-free approach to the interpretation of nuclear magnetic resonance relaxation in macromolecules. *J Am Chem Soc* **104**: 4546–4570.

Ochsenbein F, Neumann JM, Guittet E, van Heijenoort C (2002) Dynamic characterization of residual and nonnative structures in a partially folded protein by ^{15}N NMR relaxation using a model based on a distribution of correlation times. *Protein Sci* **11**: 957–964.

Palmer AG (2004) NMR characterization of the dynamics of biomolecules. *Chem Rev* **104**: 3623–3640.

Parsons L, Eisenstein E, Orban J (2001) Solution structure of HI0257, a bacterial ribosome binding protein. *Biochemistry* **40**: 10979–10986.

Peng JW, Wagner G (1995) Frequency spectrum of NH bonds in eglin C from spectral density mapping at multiple fields. *Biochemistry* **34**: 16733–16752.

Press WH, Flannery BP, Teukolsky SA, Vetterling WT (1986) *Numerical recipes. The art of scientific computing*; pp 529–538. Cambridge University Press, Cambridge.

Rak A, Kalinin A, Shcherbakov D, Bayer P (2002) Solution structure of the ribosome-associated cold shock response protein Yfia of *Escherichia coli*. *Biochem Biophys Res Commun* **299**: 710–714.

Shaka A, Baker PB, Freeman R (1985) Computer-optimized decoupling scheme for wideband applications at low-level operation. *J Magn Reson* **64**: 547–552.

Stone MJ, Fairbrother WJ, Palmer III AG, Reizer J, Saier Jr. MH, Wright PE (1992) Backbone dynamics of the *Bacillus subtilis* glucose permease IIA domain determined from ^{15}N NMR relaxation measurements. *Biochemistry* **31**: 4394–4406.

Tjandra N, Kuboniwa H, Bax A (1995) Rotational dynamics of calcium-free calmodulin studied by ^{15}N-NMR relaxation measurements. *Eur J Biochem* **230**: 1014–1024.

Tjandra N, Szabo A, Bax A (1996a) Protein backbone dynamics and ^{15}N chemical shift anisotropy from quantitative measurement of relaxation interference effects. *J Am Chem Soc* **118**: 6986–6991.

Tjandra N, Wingfield P, Stahl S, Bax A (1996b) Anisotropic rotational diffusion of perdeuterated HIV protease from ^{15}N NMR relaxation measurements at two magnetic fields. *J Biomol NMR* **8**: 273–284.

Vila-Sanjurjo A, Schuwirth BS, Hau CW, Cate JHD (2004) Structural basis for the control of translation initiation during stress. *Nat Struc Mol Biol* **1**: 1054–1059.

Ward IM, Klein PG (1996) Polymer physics. In *Encyclopedia of nuclear magnetic resonance.* Grant DM, Harris RK, eds, pp 3693–3706, Wiley, Chichester.

Woessner DE (1962) Nuclear spin relaxation in ellipsoid undergoing rotational Brownian motion. *J Chem Phys* **37**: 647–654.

Ye K, Serganov A, Hu W, Garber M, Patel DJ (2002) Ribosome-associated factor Y adopts a fold resembling a double-stranded RNA binding domain scaffold. *Eur J Biochem* **269**: 5182–5191.

Zhukov I, Ejchart A (1999) Factors improving the accuracy of determination of ^{15}N relaxation parameters in proteins. *Acta Biochim Polon* **46**: 665–671.